Alpha-motoneurons maintain biophysical heterogeneity in obesity and diabetes in Zucker rats.

Christopher W. MacDonell, Jeremy W. Chopek, Kalan R Gardiner, Phillip F Gardiner

Spinal Cord Research Centre, Department of Physiology & Pathophysiology, Rady Faculty of Health, University of Manitoba, Winnipeg, MB, R3E 0J9

Abbreviated Title: Obese and diabetic motoneurons

Keyword: motoneuron, obesity, diabetes, electrophysiology, neurophysiology.

Correspondence to:
Christopher W. MacDonell, Ph.D.
402 Basic Medical Science Building
Spinal Cord Research Centre, Department of Physiology & Pathophysiology, Faculty of Medicine,
University of Manitoba
Winnipeg MB, Canada, R3E 0J9
Telephone: 204.977.5622
Facsimile: 204.789.3930
Email: cmacdon@scrc.umanitoba.ca

ABSTRACT

Small diameter sensory dysfunction resulting from diabetes has received much attention in the literature, while the impact of diabetes on alpha-motoneurons (MN) has not. In addition to this, the chance of developing insulin resistance and diabetes is increased in obesity. No study has examined the impact of obesity or diabetes on the biophysical properties of MN. Lean Zucker rats and Zucker Diabetic Fatty (ZDF) rats were separated into Lean, Obese (ZDF fed standard chow) and Diabetic (ZDF fed high fat diet that led to diabetes) groups. Glass micropipettes recorded hind-limb motoneuron properties from identified flexor and extensor motoneurons. Motoneurons were separated within their groups based on input conductance, which created high and low input conductance subpopulations for each. A significant shorter (20%) afterhyperpolarization half-decay (AHP1/2) was found in low conductance motoneurons for the diabetic group only, while the AHP1/2 tended to be shorter in the Obese group (19%). Significant positive correlations were found among Rheobase and input conductance for both lean and obese animals. No differences were found between the groups for the afterhyperpolarization amplitude (AHPamp), input conductance (IC), rheobase or any of the rhythmic firing properties (Frequency-Current slope and spike frequency adaptation index). Motoneuron properties continue to be heterogeneous in obese and diabetic animals. Obesity does not seem to influence lumbar motoneurons. Despite the motoneurons resistance to the impact of diabetes, the reduced AHP ½ decay and the tendency for a reduction in AHPamp may be the first sign of change to motoneuron function.

NEW & NOTEWORTHY

Knowledge about the impact of obesity and diabetes on the biophysical properties of motoneurons is lacking. We found that diabetes reduces the duration of the afterhyperpolarization and that motoneuron function is unchanged by obesity. A reduced afterhyperpolarization may impact discharge characteristics and may be the first sign of change to motoneuron function.

INTRODUCTION

Health concerns related to obesity and diabetes are growing. In Canada, adults that are overweight or obese (BMI greater than 25) constitute 54% of the population (Statistics Canada, 2014). Further to this, obesity is associated with increased risk of developing diabetes in persons greater than 18 years of age (Millar and Young, 2003). It has been shown by many that diabetes disrupts the normal physiological function of small-diameter sensory nerves over time, leading to increased pain and/or loss of sensation (see review, Duby et al. 2004). However, there are few studies that have examined how diabetes affects alpha-motoneurons (hereafter referred to as motoneuron) in the lumbar spinal cord.

A properly functioning sensory system seems to be necessary for producing optimal motor output. In a spinal transected animal model, with either reduced or eliminated sensory feedback, basic and rhythmic lumbar motoneuron properties show less excitability (Button et al. 2008; Beaumont et al. 2004). However, when spinal transected rats go through a passive cycling exercise regime, proper spinal motoneuron function is restored (Beaumont et al. 2004). Part of this restoration in function may be due to the sensory feedback created by the movement of the lower limbs. As such, any change in small diameter sensory afferents via diabetes, may impact motoneuron output.

In humans, studies have shown that motor units from limb muscles in both Type I and II diabetics show deficits when compared to non-diabetics. Motor axons were shown to have a decreased conduction velocity, while compound muscle action potentials were smaller in amplitude and longer in duration in

diabetics (Brown and Feasby, 1974; Hansen and Ballantyne, 1977). In addition, motor unit number estimates showed estimated decreases in the thenar and extensor digitorum brevis muscles of adult diabetics (Brown and Feasby, 1974); a finding that has been confirmed in additional muscles in adults (Hansen and Ballantyne, 1977; Allen et al. 2013;) and type I diabetic children (Toth et al. 2014). Functionally, motor unit firing rates, peak force production and time to fatigue parameters were reduced in human Type I diabetics (Almeida et al., 2008); while in type II diabetics, both motor unit firing rate and the stability of the force signal was reduced during isometric contraction (Watanabe et al. 2013). Finally, a redistribution of muscle fiber type to a fast-twitch phenotype has been shown to occur as a result of diabetes (Oberbach et al. 2006).

In Type I diabetic rodent models, similar changes in the neuromuscular system have been found. Following streptozotocin (STZ) injection (Type I diabetes model), mice showed a decrease in motor unit number estimates, increased single motor unit potentials (Souayah et al. 2009), decreased motor axonal conduction velocity, and reduced compound muscle action potential (CMAP) amplitude (Ramji et al. 2007). In addition, neuromuscular junction numbers were reduced by 60% (Ramji et al. 2007) and miniature endplate current amplitudes and acetylcholine quantal release were reduced in response to 1-Hz nerve stimulation (Souayah et al. 2009). In Type II diabetic rodents, the Zucker Diabetic Fatty rat (ZDF) model suffers from slowed motor nerve (Coppey et al., 2002) and sensory nerve conduction velocity, as well as decreased CMAP and sensory nerve action potential amplitudes (Russell et al. 2008). While Type I myosin heavy chain (MHC) content decreases, fast Type II MHC content increases (Kim et al. 2015). Finally, changes to thermal and mechanical nociception occur (Sugimoto et al., 2008).

At the spinal motoneuron and motor nuclei level, available literature suggests that diabetes may impact motor nuclei size and number. Dorfman et al., (2004) found a decrease in spinal nuclei volume and a shift towards smaller nuclei area in the bulbocavernosuous motor nucleus of induced diabetic rats (4

93 weeks post STZ). However, Ramji et al. (2007) found no difference in either the number or
94 morphological characteristic of motor nuclei in the lumbar spinal cord of mice (8 months post STZ) but
95 did find an increase in cellular markers of neuronal stress and protection. In addition, Muramatsu et al.,
96 (2011) found that both size and number of presumed gamma-motoneurons were reduced (22-weeks
97 post STZ) in rats, but later reported (Muramatsu et al., 2017) that large (presumed alpha) and small
98 motoneurons of the MG nucleus had less cross-sectional area (12 weeks post) and were fewer in
99 number (12 and 24 weeks post STZ). Although slightly variable, the balance of results from the available
100 literature suggests motoneurons are susceptible to the effects of diabetes in a Type I diabetic model.

101 A strong association exists between obesity and insulin resistance that leads to type II diabetes,
102 which is likely mediated by widespread chronic inflammation (Hotamisligil et al. 1993; Hotamisligil,
103 2006). Given the association between obesity and diabetes, any change in motoneuron function may
104 exist along a continuum and therefore be evident in obese non-diabetics. In the ZDF model, decreased
105 oxidative capacity and increase in fast Type II muscle fibers have been found compared to control rats
106 (Acevedo et al., in press). In humans, with regard to obesity and the neuromuscular system, the
107 reported impact of being overweight or obese on motoneuron function is limited to voluntary activation
108 assessed via the twitch interpolation technique and muscular strength. Blimkie et al. (1990) showed
109 voluntary activation in adolescent obese males to be lower during isometric knee extensor contractions
110 compared to age-matched lean adolescents. In contrast, Garcia-Vicencio et al. show that adolescent
111 girls have increased voluntary activation of knee extensors during fatiguing isometric contractions
112 (2015) and during isometric contractions (2016) in both knee extensor and plantar flexor muscle groups.
113 In addition, greater absolute knee extensor strength has been shown in obese adolescent males
114 (Abdelmoula et al., 2012) and females (Garcia-Vicencio et al. 2015) compared to lean individuals, while
115 relative strength has been shown to be higher (Abdelmoula et al., 2012) less (Maffiuletti et al., 2008) or
116 similar (Blimkie et al. 1990) compared to lean adolescents. Relative plantar flexor strength has been

117 evaluated only in females and was recently shown to be greater in obese adolescent girls (Garcia-
118 Vicencio et al. 2016). Although variable, these results may imply that increased body mass may confer
119 a neuromuscular overload effect consistent with changes seen in the neuromuscular system as a result
120 of increased activity in an animal model (wheel and treadmill running; Beaumont and Gardiner, 2002;
121 2003).

122 Healthy motoneurons have distinct heterogeneous properties that operate over a continuum and relate
123 to the type of muscle fiber innervated. For example, motoneuron afterhyperpolarization amplitude and
124 duration are greater, rheobase current is less, and input resistance is larger in motoneurons that
125 innervate slow twitch muscle fibers compared to those that innervate fast twitch muscle fibers (Eccles et
126 al. 1958; Gardiner and Kernell, 1990; Zengel et al. 1985; Fleschman et al. 1981). Motoneuron
127 biophysical properties are also not static and respond to exercise (Beaumont and Gardiner, 2002, 2003;
128 Beaumont et al. 2004; MacDonell et al., 2012), sedentary activity (Cormery et al. 2005), as well as
129 eliminated descending and afferent input (Button et al., 2008). To our knowledge, no studies have
130 examined the impact of diabetes or obesity on motoneuron biophysical function. The purpose of this
131 investigation was to establish the impact of diabetes and obesity on flexor and extensor lumbar
132 motoneurons in diabetic and obese rats. Given the reported changes in motor units and reduced
133 motoneuron number and area (Muramatsu et al. 2017; Dorfman et al., 2004), altered
134 electrophysiological properties mentioned above should be evident from the sampled motoneuron
135 pool. In addition, with obesity, the extra mass may confer a training overload effect that would
136 translate to changes in motoneuron properties similar to that seen with exercise trained rats (Beaumont
137 and Gardiner, 2002, 2003).

METHODS

Experimental Animals

Female Zucker Diabetic Fatty (ZDF) and Zucker Lean rats were received from Charles River at six weeks of age. The animals were divided into three groups: 1) Zucker Lean (Lean) group that were fed standard chow, 2) Zucker Obese (Obese) group that were of the ZDF strain but were fed standard chow and 3) Zucker Obese-Diabetic (Diabetic) group that were fed a high fat diet (D12468, Research Diets Inc., NJ, USA) that has been shown to consistently induce a diabetic phenotype (Mulder et al., 2010). Rats were caged in pairs in the Animal Care facility at the University of Manitoba.

A subset of animals had their blood glucose tested (Table 1) at the beginning of the experiment, immediately after induction of a surgical plane using a mixture of Isoflurane (5%) and pure oxygen. Following induction, anesthesia was maintained (1-2.5% Isoflurane), and verified by monitoring heart rate and testing bilateral toe-pinch and eye-lash reflexes. Isoflurane delivery occurred until the completion of a precollicular-postmamillary decerebration, after which ventilation of the animal occurred with pure oxygen until the termination of the experiment. The animals had a mean age of 9.2 months at the time of data collection. In accordance with the University of Manitoba animal ethics, at the termination of data collection, animals were killed by an IV injection of potassium-chloride and a bilateral pneumothorax. The authors confirm that the present research was carried out in accordance to the animal ethics committee for the University of Manitoba, which met the guidelines set forth by the Canadian Council of Animal Care.

Surgical Procedures

Immediately following the induction of anaesthesia and glucose testing, an IP injection of atropine (0.05 $mg \cdot kg^{-1}$ atropine within 5% dextrose physiological saline) was administered to minimize airway secretions. Following atropine administration bilateral toe-pinch reflexes were re-assessed to

ensure the animal was in a surgical plane of anaesthesia. The surgical procedures, in order included: 1) left tibial (extensor) and peroneal (flexor) nerves exposure for antidromic stimulation, 2) insertion of a tracheal tube for ventilation (Harvard Apparatus, CA; rate: 60-80 strokes min^{-1}; tidal volume range 2.0 to 2.5 mL), and expired CO_2 monitoring (levels ranged 3-4%; CAPSTAR 100 CO_2 analyzer, CWE Inc., USA); 3) cannulization of the right carotid artery to monitor mean arterial blood pressure (MAP) and provide an infusion port; 4) dexamethasone administration (0.1 mL) via the carotid artery cannula to reduce swelling of the brain; 5) occlusion of left carotid with a suture (2-0) prior to dissection of the back musculature in preparation for a laminectomy (T12 to S1); and 6) laminectomy within a stereotaxic frame. Upon completion of the laminectomy, the dorsal roots were brushed aside, a mineral oil bath was formed and the parietal bones of the skull were exposed and excised to prepare for a precollicular-postmamillary decerebration.

In an attempt to reduce bleeding, both carotid arteries were previously tied off. The skull was removed bilaterally, leaving the central and inter-parietal sutures intact. This resulted in small oval holes in the skull superior to the zygomatic arches with the inter-parietal suture, the central suture and 2mm rostral of bregma as the borders. The sutures and dura were cauterized to reduce bleeding. Under low suction the cortex was removed in the parietal regions while controlling bleeding with a combination of Surgicel, (Johnson and Johnson USA); Instat, (Johnson and Johnson, USA); Gelfoam, (Pharmacia and Upjohn, USA); and Surgi absorbent swabs, (Kettenbach GmbH and Co., DE). The remaining skull along the central suture was removed and the remaining tissue was aspirated until the superior colliculi and thalamus were exposed. At this point, a pre-collicular cut was made and the hypothalamus, thalamus, and forebrain removed. Absorbable hemostat was applied to control bleeding throughout the procedure. Typically, MAP decreased to 50 mmHg during the procedure, but rebounded to 80 mmHG or more within minutes. However, if MAP did not restore due to excessive hemorrhaging, a saline-alginate (0.07%) solution was administered intravenously to expand plasma volume and restore MAP (Cabrales

et al. 2004). Following decerebration, isoflurane delivery was discontinued and the animal ventilated with pure oxygen for data collection. To eliminate movement of the animal from antidromic stimulation of the peripheral nerves a neuromuscular junction blocker (Pancuronium bromide, 2mg/mL) was administered to paralyze the animal and a unilateral pneumothorax helped reduce movement of the spinal cord related to ventilation. Following the pneumothorax, both tibial and peroneal nerves were mounted using silver-chloride hook electrodes and the micropipette was positioned along the L3-L4 dorsal root.

Intracellular Recordings

Glass micropipettes (1.0 mm thin-walled, World Precision Instruments, USA) were formed with a 1-2 μm diameter (resistance 7 – 12 MΩ; Kopf Vertical Pipette Puller, David Kopf Instruments, USA) and filled with a two-molar solution of K+ Citrate. The use of bilateral flexor (peroneal) and extensor (tibial) silver-chloride hook electrodes allowed for peripheral nerve stimulation to identify spinal motoneurons antidromically. Stimulation of the peroneal and tibial nerves occurred at a frequency of 2 – 3 Hz (0.1-0.2 mA for 0.1 ms) whereby the field potentials produced were monitored continuously during micropipette advancement through the spinal cord. Intracellular motoneuron records were collected at 20 KHz by an Axoclamp intracellular amplifier system (Axoclamp 2B, Axon Instruments Inc., USA) used either in bridge or discontinuous current-clamp mode (DCC; 3-10 kHz switching), with capacitance maximally compensated. Evidence of successful motoneuron impalement included a sudden increase in membrane potential to at least 50 mV, an antidromic action potential (AP) spike amplitude greater than 55 mV with a positive overshoot and a reproducible latency of less than 2.5 ms from the stimulation artifact. Upon completion of data collection from a motoneuron, confirmation of the resting membrane potential occurred by backing the micropipette out of the cell using steps of five-μm.

Intracellular Data

The following intracellular data were collected in DCC mode (3-8 kHz) from antidromically identified hindlimb motoneurons: 1) rheobase, defined as the current amplitude of a 50-ms depolarizing pulse that caused an action potential 50% of the time; 2) input conductance, defined as the reciprocal of the motoneuron input resistance calculated from the average membrane response to 25 or more 150-ms 1-nA hyperpolarizing current pulses, 3) the discharge response to a ten-second triangular depolarizing ramp current injection, to calculate the frequency-current (F/I) slope to slow input; 4) a series of 500-ms depolarizing current pulse injections to calculate the F/I slope to a fast input and 5) an adaptation index from the F/I slope calculated from the reciprocal of the averaged last 3 ISI to the first ISI (see below). In addition, resting membrane potential was measured before a short 0.5 ms intracellular depolarizing pulse in bridge mode. An average of at least 30 of the resulting action potentials, the afterhyperpolarization (AHP) amplitude (AHPamp), AHP half-decay ($AHP_{1/2}$), spike height, and spike duration were measured. Except for the adaptation index and frequency-current slope relationship (described below), the groups were subdivided into high and low conductance subpopulations based on the 50^{th} percentile value of each group (Figure 1) Those motoneurons with an IC greater than the 50^{th} percentile were designated as high input conductance motoneurons, while those less than or equal to the 50^{th} percentile were designated as low input conductance motoneurons.

Frequency-Current Relationship Slope

The slope of the frequency current (F/I) relationship was calculated by applying linear regression to the data obtained from a slow depolarizing triangular (5-s ascending and 5-s descending) intracellular current injection and a fast depolarizing (500-ms) intracellular current injection.

Slow depolarizing triangular current injection (slow F/I): The reciprocal of the inter-spike interval from action potentials produced by current injection were plotted against current amplitude to obtain the slow F/I relationship, wherefrom the slow F/I slope was calculated.

500-ms depolarizing current injection (fast F/I): A series of increasing amplitude 500-ms depolarizing current steps were delivered (0.3 Hz) until the motoneuron failed to discharge the entire 500-ms epoch. The reciprocal of the first inter-spike interval produced from each current step (with exception of the step where discharge failed) was plotted against the current amplitude to obtain the F/I relationship, wherefrom the fast F/I slope was calculated.

Spike Frequency Adaptation Index

Spike frequency adaptation (SFA) is the time dependent decrease in discharge rate during a constant depolarizing current injection (Granit et al. 1965). SFA was assessed by creating an index of the F/I slopes calculated from the initial firing frequency and steady-state firing frequency of the action potentials collected during a series of 500-ms depolarizing current injections. The initial firing frequency comprised the first two spikes (Initial), while the steady-state firing frequency (SSFF) contained the last four spikes. As done previously (MacDonell et al., 2012), the ratio of the SSFF F/I slope to the Initial F/I slope yielded the SFA adaptation index (AI).

Statistics

All statistical tests were computed in MATLAB (R2013a, Mathworks Inc., MA) and figures were created with Origin (version 7, OriginLab Corp., MA). The first step in statistical analysis was to determine whether the dependent variables were distributed normally. For the normality test and subsequent analyses, a p-value of less than or equal to 0.05 determined significance.

The following variables were found to be not normally distributed according to the Kolmogorov-Smirnov normality test: $AHP_{1/2}$, AHPamp, AI, IC, rheobase, fast F/I and slow F/I (p-values < 0.0001). Due to the decision to separate the motoneurons into high and low conductance groups, the Kolmogorov-Smirnov two sample test was used to determine if the distribution of IC values were different between the groups. The Kolmogorov-Smirnov test returned non-significant probability values for each comparison (Lean-Obese, p = 0.184; Lean-Diabetic, p = 0.452; Obese-Diabetic, p = 0.1334).

Given the above, non-parametric statistics were chosen to determine if differences existed between Lean, Obese and Diabetic hindlimb motoneuron properties. Kruskal-Wallis analysis of variance (KW-ANOVA) on ranks tested whether the dependent variables (see above) were significantly different between the groups (Lean, Obese and Diabetic) but is limited to one level. Ranksum tests evaluated which groups differed following a significant KW-ANOVA test and were also used to determine significance between two groups. Spearman's Rho (ρ) tested the magnitude and direction of any correlation between variables.

Differences between groups for mass and blood glucose levels were tested with parametric tests. Significant differences were tested with separate one way independent ANOVA. Upon finding a significant result, a student's t-test tested for any differences in means between the groups. Since the variances between the groups were unequal, the unequal variance t-test determined the t-critical value. The increase in familywise error rate due to multiple comparisons was not corrected for because it was deemed that avoiding a type II error (failing to reject the null hypothesis when it should have been rejected) was more important than inflating the type I error rate (rejecting the null hypothesis instead of failing to reject the null hypothesis). Data are presented as the median with the interquartile range (IQR) in brackets for non-parametric data and mean (SD) for parametric data.

RESULTS

In total, data were collected from 195 hindlimb motoneurons from 50 animals (17 Lean; 17 Obese; 16 Diabetic). Motoneuron properties were collected from both flexor and extensor motoneuron pools. No significant difference between motoneuron pools was evident. Therefore, flexor and extensor data was pooled. Average mass and glucose levels for each group are displayed in Table 1. Significant main effects for mass ($F_{(2,45)} = 3.2$, $p < 0.00001$) and blood glucose levels ($F_{(2,18)} = 3.5$, $p = 0.00013$) were found. For blood glucose, all groups had a significantly different blood glucose level, where Lean (7.3 $mmolL^{-1}$) <

Obese (10.2 $mmolL^{-1}$) < Diabetic (20.5 $mmolL^{-1}$) ($p < 0.001$). For mass, Obese (359 g) and Diabetic (367 g) animals had a similar mean mass, but both were heavier than lean (249 g) animals ($p < 0.00001$).

Figure 1 shows the cumulative distribution of the input conductance for each group, and the 50^{th} percentile cut-off that separated the data into high and low conductance motoneuron groups. Those cells with an IC above the 50^{th} percentile was categorized as high IC cells, while those at or below the 50^{th} percentile was categorized as low IC cells. Table 2 contains median (IQR) biophysical properties for hindlimb motoneurons. Median values for IC, AI, fast F/I, slow F/I, and rheobase were found to be similar, whereas the AHP1/2 was shorter in low conductance cells in diabetic animals compared to control.

Figure 2 illustrates the AHP1/2 decay and amplitude for high IC and low IC motoneurons in each of the three groups. The AHPamp and AHP1/2 for high IC cells showed no difference and the AHPamp of low conductance cells tended to be smaller in amplitude ($p=0.067$). Significant main effects were found for the AHP1/2 ($\chi^2_{(2, 76)} = 7.73$, $p = 0.021$) in low conductance cells (Figure 3), whereby a longer duration AHP1/2 was found in the Lean (15.35 ± 6.9) group compared to the Diabetic group (12.3 ± 3.8; $Z = 2.67$, $p = 0.0076$). The AHP1/2 of the Obese (12.5 ± 8) group tended to be shorter than the lean group ($p = 0.065$), but did not differ from the Diabetic group. When motoneurons are separated into low IC and high IC regardless of experimental group, the low IC group had a greater AHPamp (1.7 mV $\pm$ 3.1 vs 1.2 mV $\pm$ 0.55; $p = 0.018$) and AHP1/2 durations (15.3 ms $\pm$ 6.9 vs 12.2 $\pm$ 2.8; $p = 0.0009$) than those of high input conductance cells.

Moderate positive correlations (Figure 4) between IC and rheobase were found for Lean ($\rho= 0.65$, $p < 0.00001$), Obese ($\rho= 0.46$, $p = 0.003$) and Diabetic ($\rho= 0.51$, $p = 0.0002$) animals, indicating that the relationship between excitability and ion conductance was not appreciably altered in the experimental groups. Significant moderate negative correlations were also shown for Lean ($\rho= -0.51$, $p = 0.00001$) and

Obese (ρ = -0.39, p = 0.0109) animals for the relationship between AHP1/2 and IC, while Diabetic (ρ = -0.14, p = 0.3257) animals showed no correlation between AHP1/2 and IC (Figure 5). Diabetic animals seem to lack the same number of long duration AHP1/2, compared to that seen in the Lean and Obese animals, despite having a similar range of IC.

DISCUSSION

This investigation is the first to report on biophysical motoneuron properties in diabetic and obese animals. The main finding of this investigation is spinal lumbar motoneurons are not appreciably impacted by diabetes or obesity, showing that motoneurons maintain their biophysical heterogeneity. A decrease in the half-decay duration of the afterhyperpolarization in diabetic animals was the only difference found among the animals and is discussed below. The finding that all other properties measured were similar across groups suggests that changes in motor unit physiology are not necessarily due to a widespread change in function of motoneurons, at least at the level of the lumbar spinal cord. These finding do not preclude changes to motoneuron morphology but does indicate that most electrophysiological parameters remain intact in the Zucker Type II diabetes model. As for obese rats, motoneurons were not impacted by increased body mass.

Afterhyperpolarization

This investigation found the afterhyperpolarization half-decay to be reduced in Diabetic rats (3-ms median reduction) and a tendency for the amplitude to be reduced in Diabetic animals (0.6 mV median reduction). When the motoneuron is driven to fire action potentials via depolarizing current injections, the AHP duration is correlated to the cells minimum rate of discharge (Kernell, 1965) and to the type (fast or slow) of motoneuron (Eccles et al. 1958; Gardiner 1993). When the motoneuron is driven to fire by way of mesencephalic locomotor region stimulation, the AHP is largely reduced (cats and rats) and motoneuron firing is more variable (Brownstone et al. 1992; MacDonell e al. 2015). These two scenarios, discharge during quiescence and discharge during motor output, represent two highly

different states of synaptic drive but the average discharge rate between the two scenarios has been found to be similar (Brownstone et al. 1992), suggesting that the AHP may not govern discharge during motor behaviour. The faster AHP1/2 in diabetic motoneurons found herein, may represent a transition to more excitable state. This could allow for faster motoneuron discharge at lower levels of drive (a reduced AHP is known to increase the gain of the motoneuron; Lape and Nistri, 2000; Miles et al. 2007) and impact the ability of the motoneuron to maintain low rates of firing during fine motor movements/ low synaptic drive.

Another possibility is that muscle remodelling influenced the afterhyperpolarization duration of the innervated muscle unit. While fiber-type distribution was not measured in this study, a shift in fiber type distribution in human and animals has been shown. Humans with non-insulin dependent type II diabetes show increased Type IIx muscle fibers and decreased Type I muscle fibers compared to control (Marin et al., 1994; Oberbach et al., 2006). In both ZDF (Kim et al. 2015) and STZ rats (Snow et al. 2005), increases in Type II MHC (associated with fast type muscle fibers) and decreases in the Type I MHC (associated with slow type muscle fibers) compared to control rats have been shown to occur by 12 (STZ) and 13 weeks (ZDF). Finally, Russell et al. (2008) showed decreased sensory nerve conduction velocities, CMAP amplitudes and sensory nerve synaptic potential amplitudes following 10 weeks of hyperglycemia. Muscle and sensory changes documented above, all occurred before the mean age (36.8 weeks) of the ZDF rat used in the current study.

If there were a similar re-organization of fiber type in the diabetic animals, motoneurons may have adapted to the change in phenotype due to the speed-match that exists between motoneurons and the muscle fibers they innervate (Gardiner and Kernell, 1990; MacDonell et al. 2008). A retrograde influence of muscle on motoneuron AHP following muscle denervation/reinnervation has been demonstrated (Foehring and Munson, 1990). In these experiments, Foehring and Munson (1990) cross-innervated the

medial gastrocnemius and soleus nerves. The electrical properties of the medial gastrocnemius motoneuron pool innervating the soleus muscle changed and became more *slow-like*. That is, the AHP duration and input resistance increased and rheobase decreased. In addition, Cormery et al. (2000) showed that AHP durations in slow motoneurons are shorter in rats after four weeks of tetrodotoxin induced hindlimb paralysis. A change in muscle phenotype, therefore, may explain the change in AHP, if a change in fiber type distribution occurred.

We used the input conductance 50th percentile value to separate the groups into high and low input conductance subpopulations. This was done to ensure a change in the AHP parameters was not missed, given that the AHP is mutable (Gardiner and Beaumont, 2002; 2003; Cormery et al. 2003). Had we used the AHP ½ duration criteria to separate putative fast and slow motoneuron types used by Gardiner (1993), any change in AHP may have been masked. Since the cumulative distribution of the input conductance between Lean, Obese, and Diabetic groups did not differ (Figure 1.), and input conductance is a robust measure that relates well with motoneuron type (Zengel et al., 1985), it provided a way to compare motoneurons without missing any potential change in AHP parameters.

Unchanged motoneuron properties in diabetic animals

In a Type I diabetic animal model, Ramji et al. (2007) showed little change to motoneuron morphology or number in the lumbar spinal cord but that the tibialis anterior muscle and NMJ were adversely affected by diabetes. Similarly in a Type I diabetes model, Muramastu et al. (2012) also reported that STZ did not alter alpha-motoneuron numbers but did suggest that gamma motoneurons were lost. However, a follow-up study by the same group (Muramastu et al. 2017) showed evidence for reduced motoneuron numbers in the gastrocnemius motor nuclei at 12 and 24 weeks, with both the smallest and largest motoneurons being reduced in number, demonstrating variability in assessing motoneuron changes in diabetic models. The ZDF rat is an animal model for Type II diabetes. The ZDF rat has been shown to have elevated levels of blood glucose at 8 weeks that continues to increase up to 20 weeks

before plateauing (Sugimoto et al. 2008). In addition, at 16 weeks the ZDF rat developed an increased sensitivity to thermal nociceptive stimuli and, at 18 weeks, a decreased response to mechanical nociceptive stimuli occurred (Sugimoto et al. 2008). Other deficits, such as a decreased motor nerve conduction velocity, decreased endoneural blood flow (Coppey et al., 2002), and, as mentioned above, changes in muscle phenotype occur as early as 13 weeks in ZDF rats.

In relation to this, three reasons may be considered for the lack of widespread difference in the biophysical properties of motoneurons in our study. First, our investigation used a Type II model of diabetes, while the investigations noted above used a Type I model of disease. Second, the change in cross-sectional area and motoneuron number found by Muramastu et al., (2017), although significant, may be too modest to effect biophysical properties. Gardiner (1993) showed that rat motoneurons have a considerable range of properties that include both slow and fast motor units. Given this wide range, the effect of type II diabetes on motoneuron numbers may be too modest to detect and thus a sampling of the available motor pool reveals little difference. Third, the full impact of diabetes on spinal cord motoneurons might not be fully realized until much later. Diabetic neuropathy is polymodal and the progression of diabetic neuropathy includes changes to both peripheral nerve fibers (Dyck et al., 1986) and ion channel changes at the DRG (Hong et al., 2004). The progression of neuronal dysfunction in efferent somatic neurons may not be realized at a mean age of 9.2 months. As such, the reduced AHP ½ decay and the tendency for a reduction in AHPamp shown herein may be the first sign of change.

A probability value of 0.05 set the level of significance (i.e. Type I error rate); despite performing multiple comparisons, no adjustment to the probability value was made. As the number of comparisons increase, so does the likelihood of incorrectly rejecting the null hypothesis (false discovery). Given that this is the first report examining motoneuron biophysical properties in obese and diabetic animals, the authors chose a more liberal level of significance. Had we adjusted for the false discovery using the

equation described by Hassard and Baker (1986), an adjusted p-value of 0.026 (20 comparisons) would have been set. In relation to the data presented herein, this would have impacted only the tendency of the AHP1/2 decay to be different between Obese and Lean groups. Although adjusting the false discovery rate is an important practice, its use needs to be evaluated with the type of study being conducted.

Lack of change in obese Zucker Rats

To our knowledge, this is the first study to examine the effects of obesity on motoneuron properties. We hypothesized that the sampling distribution of electrophysiological properties may be shifted towards those properties consistent with exercised (running) motoneurons (Beaumont and Gardiner, 2002, 2003). The only relevant literature known to the authors that examined how the neuromuscular system responds to obesity looked at adolescent boys and girls. These studies suggest that the neuromuscular system adapts to obesity (Garcia-Vicencio et. al., 2015; 2016; Abdelmoula et al. 2012). In this, adolescent boys and girls tend to have increased muscle strength and total muscle activation; although there is discrepancy in the literature (Blimkie et al. 1990; Maffiuletti et al., 2008). Testing whether obesity changed motoneuron properties was important due to the association between obesity and developing Type II diabetes (Hotamisligil, 2006). The lack of a significant results found in this investigation may indicate obesity simply does not confer any benefit/detriment to motoneurons.

Conclusion

Motoneuron properties continue to be heterogeneous in obese and diabetic animals. While obesity did not influence motoneuron properties significantly, a tendency towards an altered AHP existed. Despite the motoneurons overall resilience, for diabetic neurons the reduced AHP ½ decay and the tendency for a reduction in AHPamp shown herein may be the first sign of change to motoneuron function.

FUNDING SOURCES

This research was supported by grants from the Canadian Institutes of Health Research (CIHR) Team NERVE grant and the Canada Research Chairs program. Financial support was provided by CIHR Doctoral award (J. W. Chopek).

References

Abdelmoula A, Martin C, Bouchant A, Walrand S, Lavet C, Taillardat M, Maffiuletti N, Boisseau N, Duche P and Ratel S. Knee extension strength in obese and nonobese male adolescents. Appl. Physiol. Nutr. Metab. 37: 269–275, 2012.

Acevedo LM, Raya AI, Ríos R, Aguilera–Tejero E, River JL. Obesity-induced discrepancy between contractile and metabolic phenotypes in slow- and fast-twitch skeletal muscles of female obese Zucker rats. J Appl Physio, in press,2017.

Allen MD, Choi IH, Kimpinski K, Doherty TJ and Rice CL. Motor Unit Loss & Weakness in Association with Diabetic Neuropathy in Humans. Muscle and Nerve, 48: 298-300, 2013.

Almeida S, Riddell MC, Cafarelli E. Slower conduction velocity and motor unit discharge frequency are associated with muscle fatigue during isometric exercise in type 1 diabetes mellitus. Muscle and Nerve. 37:231-40, 2008.

Button DC, Kalmar JM, Gardiner K, Marqueste T, Zhong H, Roy RR, Edgerton VR, Gardiner PF. Does elimination of afferent input modify the changes in rat motoneurone properties that occur following chronic spinal cord transection? J Physiol. 586:529-544, 2008.

Beaumont E and Gardiner P. Effects of daily spontaneous running on the electrophysiological properties of hindlimb motoneurons in rats. J Physiol 540, 129-138, 2002.

Beaumont E and Gardiner PF. Endurance training alters the biophysical properties of hindlimb motoneurons in rats. Muscle Nerve 27, 228-236, 2003.

Beaumont E, Houlé JD, Peterson CA, Gardiner PF. Passive exercise and fetal spinal cord transplant both help to restore motoneuronal properties after spinal cord transection in rats. Muscle Nerve, 29:234-242, 2004.

Blimkie CJ, Sale DG, Bar-Or O. Voluntary strength, evoked twitch contractile properties and motor unit activation of knee extensors in obese and non-obese adolescent males. Eur J Appl Physiol Occup Physiol. 61: 313-8, 1990.

Brown WF and Feasby TE. Estimates of Functional Motor Axon Loss in Diabetics. . Journal of the neurological Sciences, 1974, 23:275-293, 1974.

Brownstone RM, Jordan LM, Kriellaars DJ, Noga BR and Shefchyk SJ. On the regulation of repetetive firing in lumbar motoneruones during fictive locomotion in the cat. Exp Brain Res 90, 441-455, 1992.

Cabrales P, Tsai AG & Intaglietta M. Alginate plasma expander maintains perfusion and plasma viscosity during extreme hemodilution. *Am J Physiol*, **288**: H1708- H1716, 2005.

Coppey LJ, Gellett JS, Davidson EP, Dunlap JA, Yorek MA. Changes in endoneurial blood flow, motor nerve conduction velocity and vascular relaxation of epineurial arterioles of the sciatic nerve in ZDF-obese diabetic rats. Diabetes Metab Res Rev, 18: 49–56, 2002.

Cormery B, Marini JF, & Gardiner PF. Changes in electrophysiological properties of tibial motoneurons in the rat following 4 weeks of tetrodotoxin-induced paralysis. Neurosci Lett 287, 21-24, 2000.

Cormery B, Beaumont E, Csukly K, and Gardiner P. Hindlimb unweighting for 2 weeks alters physiological properties of rat hindlimb motoneurons. J Physiol 568, 841-850, 2005.

Dorfman VB, Vega MC, Coirini H.Reduction of the spinal nucleus of the bulbocavernosous volume by experimental diabetes. Brain Res, 1019:265-269, 2004.

Duby JJ, Campbell RK, Setter SM, White JR, Rasmussen, KA. Diabetic neuropathy: An intensive revie. American Journal of Health-System Pharmacy, 61: 160-176Granit R, Kernell D, Smith RS. Delayed depolarization and the repetitive response to intracellular stimulation of mammalian motorneurones. J Physiol 168: 890–910, 1963.

Dyck PJ, Lais A, Karnes JL, O'Brien P, Rizza R. Fiber loss is primary and multifocal in sural nerves in diabetic polyneuropathy.Ann Neurol., 19: 425-39, 1986.

Eccles JC, Eccles RM, Lundberg A. The action potentials of the alpha motoneurones supplying fast and slow muscles. J Physiol 142, 275-291, 1958.

Fleshman JW, Munson JB, Sypert GW and Friedman WA. Rheobase, input resistance, and motor-unit type in medial gastrocnemius motoneurons in the cat. J Neurophysiol 46, 1326-1338, 1981.

497 Foehring RC, Munson JB . Motoneuron and muscle-unit properties after long-term direct
498 innervation of soleus muscle by medial gastrocnemius nerve in cat. J Neurophys 64: 847-861,
499 1990.
500
501 Garcia-Vicencio S, Coudeyre E, Kluka V, Cardenoux C, Jegu AG, Fourot AV, Ratel S, Martin V. The
502 bigger, the stronger? Insights from muscle architecture and nervous characteristics in obese
503 adolescent girls. Int J Obes (Lond). 40:245-251, 2016.
504
505 Garcia-Vicencio S, Martin V, Kluka V, Cardenoux C, Jegu AG, Fourot AV, Coudeyre E, Ratel S.
506 Obesity-related differences in neuromuscular fatigue in adolescent girls. Eur J Appl Physiol. 115:
507 2421-2432, 2015.
508
509 Gardiner PF. Physiological properties of motoneurons innervating different muscle unit types in rat
510 gastrocnemius. J Neurophysiol 69, 1160-1170, 1993.
511
512 Gardiner PF and Kernell D. The "fastness" of rat motoneurones: time-course of
513 afterhyperpolarization in relation to axonal conduction velocity and muscle unit contractile
514 speed. Pflugers Arch 415, 762-766, 1990.
515
516 Hansen SH and Ballantyne JP. Axonal dysfunction in the neuropathy of diabetes mellitus: a
517 quantitative electrophysiological study. J Neurol Neurosurg Psychiatry, 40: 555-564, 1977.
518 Hassard T and Becker A. Faulty statistical analysis. J. Pediatr, 109: 1075–1076, 1986.
519
520 Hotamisligil GS. Inflammation and metabolic disorders. Nature, 444: 860-867, 2006.

Hotamisligil GS, Shargill NS, Spiegelman BM. Adipose expression of tumor necrosis factor-alpha: direct role in obesity-linked insulin resistance. Science 259, 87–91, 1993.

Hong S, Morrow TJ, Paulson PE, Isom LL, Wiley JW. Early painful diabetic neuropathy is associated with differential changes in tetrodotoxin-sensitive and -resistant sodium channels in dorsal root ganglion neurons in the rat. J Biol Chem. 279: 29341–29350, 2004.

Kalmar JM, Button DC, Gardiner K, Cahill F, Gardiner. Caloric restriction does not offset age-associated changes in the biophysical properties of motoneurons. PF. J Neurophysiol. 2009 101: 548-557, 2008.

Kernell D. The limits of firing frequency in cat lumbosacral motoneurones possessing different time course of afterhyperpolarization. Acta Physiol Scand 65, 87-100, 1965.

Kim J-Y, Choi MJ, So B, Kim H-J, Seong JK, Song W. The preventive effects of 8 weeks of resistance training on glucose tolerance and muscle fiber type composition in Zucker rats. Diabetes Metab J, 39:424-433, 2015.

Lape R , Nistri A. Current and voltage clamp studies of the spike medium afterhyperpolarization of hypoglossal motoneurons in a rat brain stem slice. J Neurophysiol 83:2987–2995, 2000.

MacDonell CW, Ivanova TD, Garland SJ. Afterhyperpolarization time-course and minimal discharge rate in low threshold motor units in humans. Exp Brain Res. 189:23-33, 2008.

MacDonell CW, Button DC, Beaumont E, Cormery B, Gardiner PF. Plasticity of rat motoneuron rhythmic firing properties with varying levels of afferent and descending inputs. J Neurophysiol. 107:265-272, 2012.

MacDonell CW, Power KE, Chopek JW, Gardiner KR, Gardiner PF. Extensor motoneurone properties are altered immediately before and during fictive locomotion in the adult decerebrate rat. J Physiol. 593:2327-2342, 2015.

Maffiuletti N, Jubeau M, Agosti F, De Col A, Sartorio A. Quadriceps muscle function characteristics in severely obese and nonobese adolescents. Eur J Appl Physiol. 103: 481-484, 2008.

Mårin P, Andersson B, Krotkiewski M, Björntorp P. Muscle fiber composition and capillary density in women and men with NIDDM. Diabetes Care, 17:382-386, 1994.

Miles GB, Hartley R, Todd AJ, Brownstone RM. Spinal cholinergic interneurons regulate the excitability of motoneurons during locomotion. Proc Natl Acad Sci USA 104: 2448–2453, 2007.

Millar WJ and Young TK. Tracking diabetes: Prevalence, incidence and risk factors. Health Reports, 14: 35-47, 2003.

Mulder GB, Luo S and Gramlich P. The zucker diabetic fatty (ZDF) rat: Diet evaluation study for the induction of type 2 diabetes in obese female ZDF rats. Charles River Technical Sheet: 1-4, 2010.

568 Muramatsu K, Niwa M, Nagai M, Kamimura T, Sasaki S, Ishiguro T. The size of motoneurons of the
569 gastrocnemius muscle in rats with diabetes. Neurosci Lett. , 531:109-113, 2012.
570
571 Muramatsu K, Niwa M, Tamaki T, Ikutomo M, Masu Y, Hasegawa T, Shimo S, Sasaki SI. Effect of
572 streptozotocin-induced diabetes on motoneurons and muscle spindles in rats. Neurosci Res.
573 115:21-28, 2017.
574
575 Toth C, Hervert V, Gougeon C, Virtanen H, Mah JK and Pacaud D. Motor unit number estimations
576 are smaller in children with type1 diabetes mellitus: A case-cohort study. Muscle and Nerve, 50:
577 593-598, 2014.
578
579 Oberbach A, Bossenz Y, Lehmann S, Niebauer J, Adams V, Paschke R, Schön MR, Blüher M, Punkt K.
580 Altered fiber distribution and fiber-specific glycolytic and oxidative enzyme activity in skeletal
581 muscle of patients with type 2 diabetes. Diabetes Care, 29:895-900, 2006.
582
583 Ohinmaa A, Jacobs P, Simpson S and Johnson JA. The projection of prevalenc and cost of diabetes in
584 Canada: 2000:2016. Canadian Journal of Diabettes, 28:1-8, 2004.
585
586 Ramji N, Toth C, Kennedy J and Zochodne DW. Does diabetes target motor neurons. Neurobiology
587 of Disease 2007, 26:301-311, 2007.
588
589 Russell JW, Berent-Spillson A, Vincent, AM, Freimann CL, Sullivan KA, Feldman EL.Oxidative injury
590 and neuropathy in diabetes and impaired glucose tolerance. Neurobiol Dis, 30:420-429, 2008.
591

Statistics Canada (2016-03-07). Body mass index, overweight or obese, self-reported, adult, by sex, provinces and territories (Percent). CANSIM, table 105-0501 and Catalogue no. 82-221-X, 2014 [Online]. http://www.statcan.gc.ca/tables-tableaux/sum-som/l01/cst01/health82b-eng.htm?sdi=body%20mass%20index, 2014.

Snow LM, Sanchez OA, McLoon LK, Serfass RC, Thompson LV. Myosin heavy chain isoform immunolabelling in diabetic rats with peripheral neuropathy. Acta Histochem, 107:221-229, 2005.

Souayah N, Potian JG, Garcia CC, Krivitskaya N, Boone C, Routh VH and McArdle JJ. Motor unit number estimate as a predictor of motor dysfunction in an animal model of type 1 diabetes. American Journal of Physiology - Endocrinology and Metabolism , 297:E602-E608, 2009.

Sugimoto K, Rashid IB, Kojimaa, K, Shoji M, Tanabe J, Tamasawa N, Suda T, Yasujima M. Time course of pain sensation in rat models of insulin resistance, type 2 diabetes, and exogenous hyperinsulinaemia. Diabetes-Metab Res, 24: 642-650, 2008.

Watanabe K, Gazzoni M, Holobar A, Miyamoto T, Fukuda K, Merletti R, Moritani T. Motor unit firing pattern of vastus lateralis muscle in type 2 diabetes mellitus patients. Muscle Nerve, 48:806-813, 2013.

Zengel JE, Reid SA, Sypert GW and Munson JB. Membrane electrical properties and prediction of motor-unit type of medial gastrocnemius motoneurons in the cat. J Neurophysiol 530, 1323-1344, 1985.

Table 1. Zucker rat mass and blood glucose level means (SD). Bold indicates a significant difference from other groups. Data are presented as mean (SD).

Table 2. Motoneuron properties separated by group. Data are presented as the median value and interquartile range (IQR) in brackets. **Bold** indicates significant from Lean $p < 0.05$. Underline indicates a tendency to differ from Lean $p < 0.07$.

Figure 1. Cumulative Distribution function (CDF) of input conductance for the groups. Input conductance (IC) for Lean (solid line), Obese (dashed line) and Diabetic (dotted line) groups are shown. The 50^{th} percentile is marked by the vertical hatched line. The 50^{th} percentile, indicated above, for each group was used to separate motoneurons into high input conductance (H-IC) and low input conductance (L-IC) cells. Those motoneurons with an IC greater than the 50^{th} percentile were designated as high input conductance motoneurons. No difference existed between the distributions of IC values between each group.

Figure 2. Post-spike afterhyperpolarization (AHP) amplitude and half-decay time. Data were separated into high and low input conductance (IC) categories according to the 50^{th} percentile of the IC for each group (see Figure 1). The AHP ½ decay time (A) and AHP amplitude (B) for the low IC are shown on the left panels, while AHP ½ decay time (C) and AHP amplitude (D) for the high IC category are displayed on the right. Whiskers represent the range of values, the 25^{th} and 75^{th} percentile are indicated by the top and bottom of the box, the median is the horizontal line within the box, while the symbol in the centre indicates the mean. * denotes significant difference from diabetic $p = 0.0026$.

Figure 3. Post-spike afterhyperpolarization (AHP) comparison between Lean and Diabetic groups. Magnified AHP tracings representative of the median value from the significantly different ($p < 0.007$) Lean (solid line) and Diabetic (dotted line) groups of low conductance cells. The inset shows the full

639 action potentials of each group (solid line, Lean; dotted line, Diabetic) generated from a supramaximal
640 orthodromic depolarizing pulse (0.5-ms).

641 **Figure 4. Rheobase versus input conductance according to groups.** Rheobase as a function of input
642 conductance for Lean (open triangle; ρ=0.65, p < 0.00001), Obese (shaded triangle; ρ=0.47, p = 0.0028),
643 and Diabetic (square; ρ=0.51, p = 0.000217) groups. Inset shows the lines of best fit for each group.

644 **Figure 5. Input conductance as a function of the afterhyperpolarization half-decay.** Spearman's rank
645 correlation coefficients for Lean (ρ = -0.51, p < 0.0001), Obese (ρ = -0.39, p = 0.01), and Diabetic (ρ = -
646 0.14, n.s.).

647

648

649 Table 1.

Measure	Mass (g)	Glucose ($mmolL^{-1}$)
Lean	**249.2 (24.2)**	**7.26 (0.9)**
Obese	358.6 (70.2)	**12.0 (6.4)**
Diabetic	367.6 (43.9)	**20.5 (4.9)**

650

651

652 Table 2.

	Lean	**Obese**	**Diabetic**
Input Conductance (10^{-6} S)	0.48 (0.2); N = 66	0.53 (0.42) N = 43	0.48 (0.28) N = 54
IC-High (10^{-6} S)	0.56 (0.16) N = 34	0.78 (0.29) N = 20	0.67 (0.18) N = 27
IC–Low (10^{-6} S)	0.33 (0.11) N = 32	0.35 (0.16) N = 23	0.39 (0.19) N = 27
Rheobase (mV)	7.2 (7.3) N = 58	7.8 (8.1) N= 40	7.5 (6.6) N = 49
Rheobase – High IC (mV)	10.25(5.8) N = 29	10.7 (5.8) N = 19	8.5 (5.3) N = 25
Rheobase –Low IC (mV)	4.75 (3.0) N = 29	4.5 (6.8) N = 21	5.6 (7.8) N = 24
AHP_{AMP} – High IC (mV)	1.22 (0.55) N = 34	1.25 (0.60) N = 20	1.19 (0.70) N = 26
$AHP_{1/2}$ – High IC (ms)	12.20 (2.8) N = 34	11.3 (2.8) N = 20	12.0 (2.4) N = 26
AHP_{AMP} – Low IC (mV)	1.8 (2.8) N = 32	1.5 (1.5) N = 22	1.2 (0.9) N = 25
$AHP_{1/2}$ – Low IC (ms)	15.35 (6.7) N = 32	12.5 (8.0) N = 22	**12.3 (3.8)** N = 25
Adaptation Index (a.u.)	0.21 (0.25) N = 25	0.15 (0.27) N = 21	0.19 (0.14) N = 27
F/I Fast	*One linear range* = 9 *Two linear ranges* = 15	*One linear range* = 9 *Two linear ranges* = 15	*One linear range* = 12 *Two linear ranges* = 16
F/I Slope (Hz·nA)	29.75 (12.43)	30.12 (24.33)	34.77 (16.35)
I_{PK} (nA)	12.87 (10.70)	11.10 (11.00)	14.96 (11.01)
I_{MN} (nA)	7.03 (7.04)	9.20 (9.59)	8.26 (11.12)
$Rate_{PK}$ (Hz)	246.31 (194.84)	187.34 (200.15)	206.19 (187.34)
$Rate_{MN}$ (Hz)	38.74 (56.27)	59.99 (84.22)	56.98 (60.88)
F/I Slow	N = 43	N = 30	N = 40
F/I Slope (Hz·nA)	9.71 (8.15)	11.05 (4.89)	10.38 (6.2)
I_{PK} (nA)	10.08 (9.76)	10.5 (8.93)	14.08 (9.14)
I_{MN} (nA)	7.17 (9.72)	7.75 (8.77)	11.28 (9.2)
$Rate_{PK}$ (Hz)	48.40 (19.34)	50.53 (29.64)	56.61 (22.30)
$Rate_{MN}$ (Hz)	10.87 (13.69)	9.54 (10.9)	9.23 (12.71)

Table 1.

Measure	Mass (g)	Glucose ($mmolL^{-1}$)
Lean	**249.2 (24.2)**	**7.26 (0.9)**
Obese	358.6 (70.2)	**12.0 (6.4)**
Diabetic	367.6 (43.9)	**20.5 (4.9)**

Table 2.

	Lean	Obese	Diabetic
Input Conductance (10^{-6}S)	0.48 (0.2); N = 66	0.53 (0.42) N = 43	0.48 (0.28) N = 54
IC-High (10^{-6} S)	0.56 (0.16) N = 34	0.78 (0.29) N = 20	0.67 (0.18) N = 27
IC–Low (10^{-6} S)	0.33 (0.11) N = 32	0.35 (0.16) N = 23	0.39 (0.19) N = 27
Rheobase (mV)	7.2 (7.3) N = 58	7.8 (8.1) N= 40	7.5 (6.6) N = 49
Rheobase – High IC (mV)	10.25(5.8) N = 29	10.7 (5.8) N = 19	8.5 (5.3) N = 25
Rheobase –Low IC (mV)	4.75 (3.0) N = 29	4.5 (6.8) N = 21	5.6 (7.8) N = 24
AHP_{AMP} – High IC (mV)	1.22 (0.55) N = 34	1.25 (0.60) N = 20	1.19 (0.70) N = 26
$AHP_{1/2}$ – High IC (ms)	12.20 (2.8) N = 34	11.3 (2.8) N = 20	12.0 (2.4) N = 26
AHP_{AMP} – Low IC (mV)	1.8 (2.8) N = 32	1.5 (1.5) N = 22	1.2 (0.9) N = 25
$AHP_{1/2}$ – Low IC (ms)	15.35 (6.7) N = 32	12.5 (8.0) N = 22	**12.3 (3.8)** N = 25
Adaptation Index (a.u.)	0.21 (0.25) N = 25	0.15 (0.27) N = 21	0.19 (0.14) N = 27
F/I Fast	*One linear range* = 9 *Two linear ranges* = 15	*One linear range* = 9 *Two linear ranges* = 15	*One linear range* = 12 *Two linear ranges* = 16
F/I Slope (Hz·nA)	29.75 (12.43)	30.12 (24.33)	34.77 (16.35)
I_{PK} (nA)	12.87 (10.70)	11.10 (11.00)	14.96 (11.01)
I_{MN} (nA)	7.03 (7.04)	9.20 (9.59)	8.26 (11.12)
$Rate_{PK}$ (Hz)	246.31 (194.84)	187.34 (200.15)	206.19 (187.34)
$Rate_{MN}$ (Hz)	38.74 (56.27)	59.99 (84.22)	56.98 (60.88)
F/I Slow	N = 43	N = 30	N = 40
F/I Slope (Hz·nA)	9.71 (8.15)	11.05 (4.89)	10.38 (6.2)
I_{PK} (nA)	10.08 (9.76)	10.5 (8.93)	14.08 (9.14)
I_{MN} (nA)	7.17 (9.72)	7.75 (8.77)	11.28 (9.2)
$Rate_{PK}$ (Hz)	48.40 (19.34)	50.53 (29.64)	56.61 (22.30)
$Rate_{MN}$ (Hz)	10.87 (13.69)	9.54 (10.9)	9.23 (12.71)

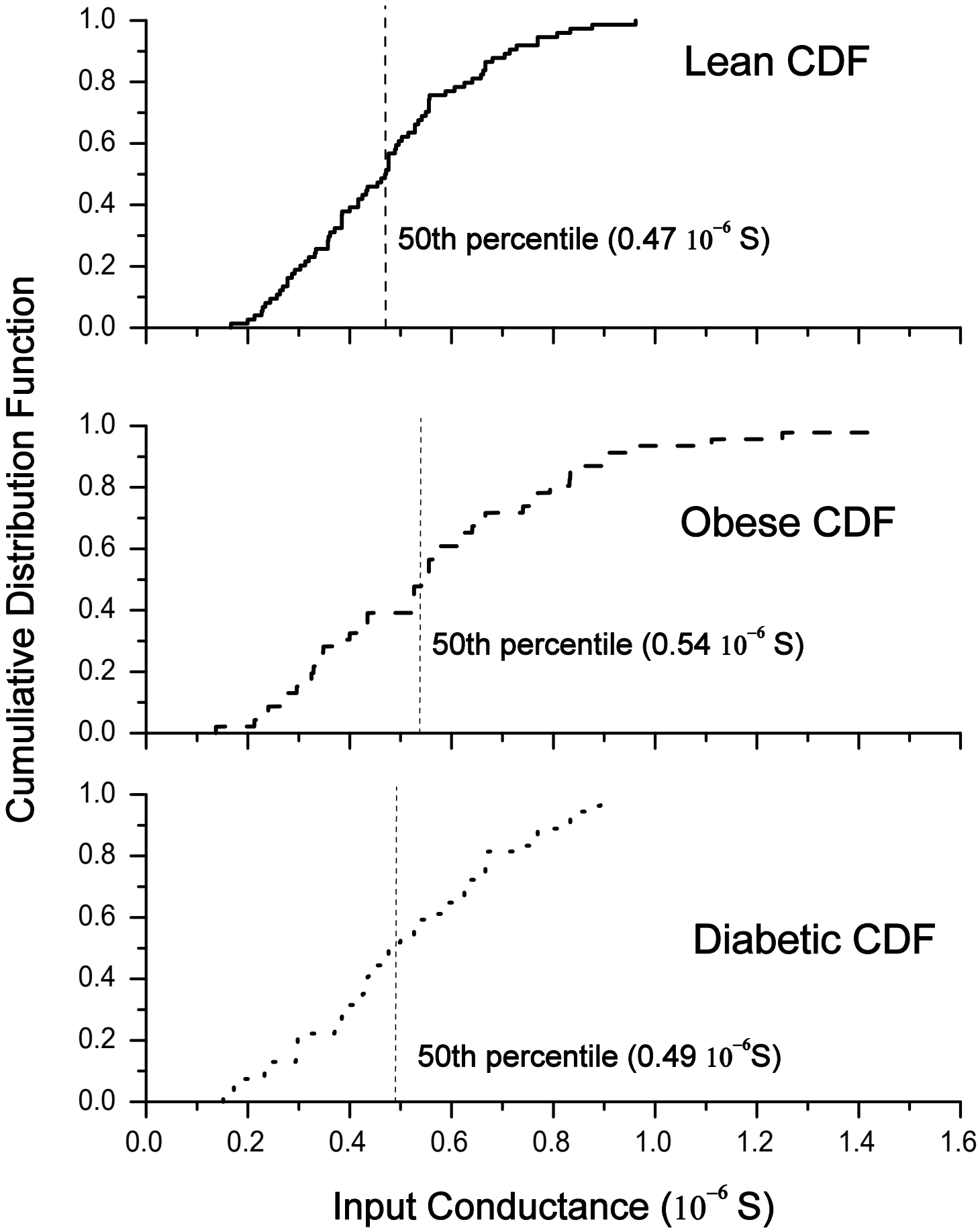
Lean CDF
50th percentile (0.47 10^-6 S)
Obese CDF
50th percentile (0.54 10^-6 S)
Diabetic CDF
50th percentile (0.49 10^-6S)
Cumulative Distribution Function
Input Conductance (10^-6 S)
0.0
0.2
0.4
0.6
0.8
1.0
1.2
1.4
1.6

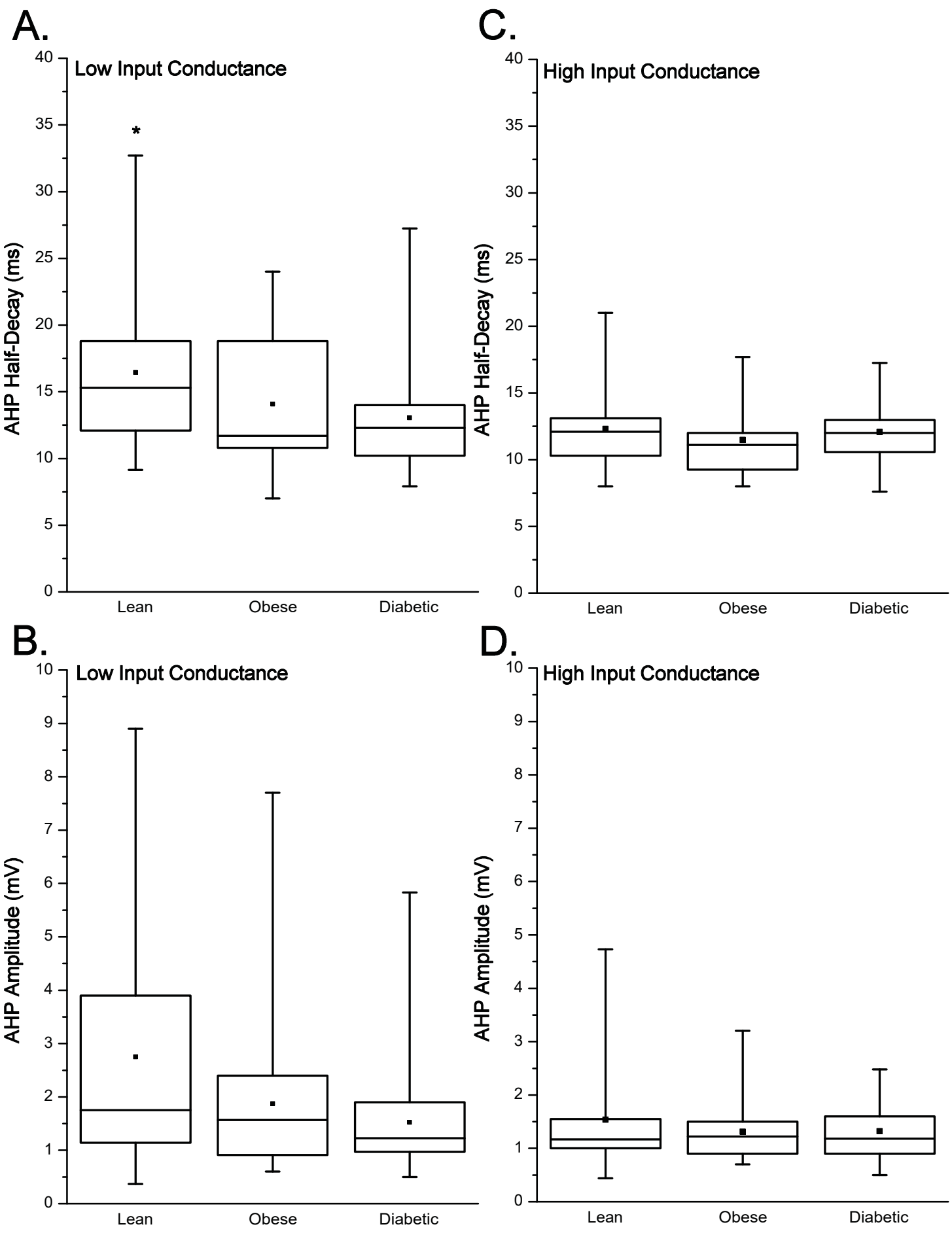
A.
Low Input Conductance
AHP Half-Decay (ms)
0
5
10
15
20
25
30
35
40
Lean
Obese
Diabetic
C.
High Input Conductance
AHP Half-Decay (ms)
0
5
10
15
20
25
30
35
40
Lean
Obese
Diabetic
B.
Low Input Conductance
AHP Amplitude (mV)
0
1
2
3
4
5
6
7
8
9
10
Lean
Obese
Diabetic
D.
High Input Conductance
AHP Amplitude (mV)
0
1
2
3
4
5
6
7
8
9
10
Lean
Obese
Diabetic

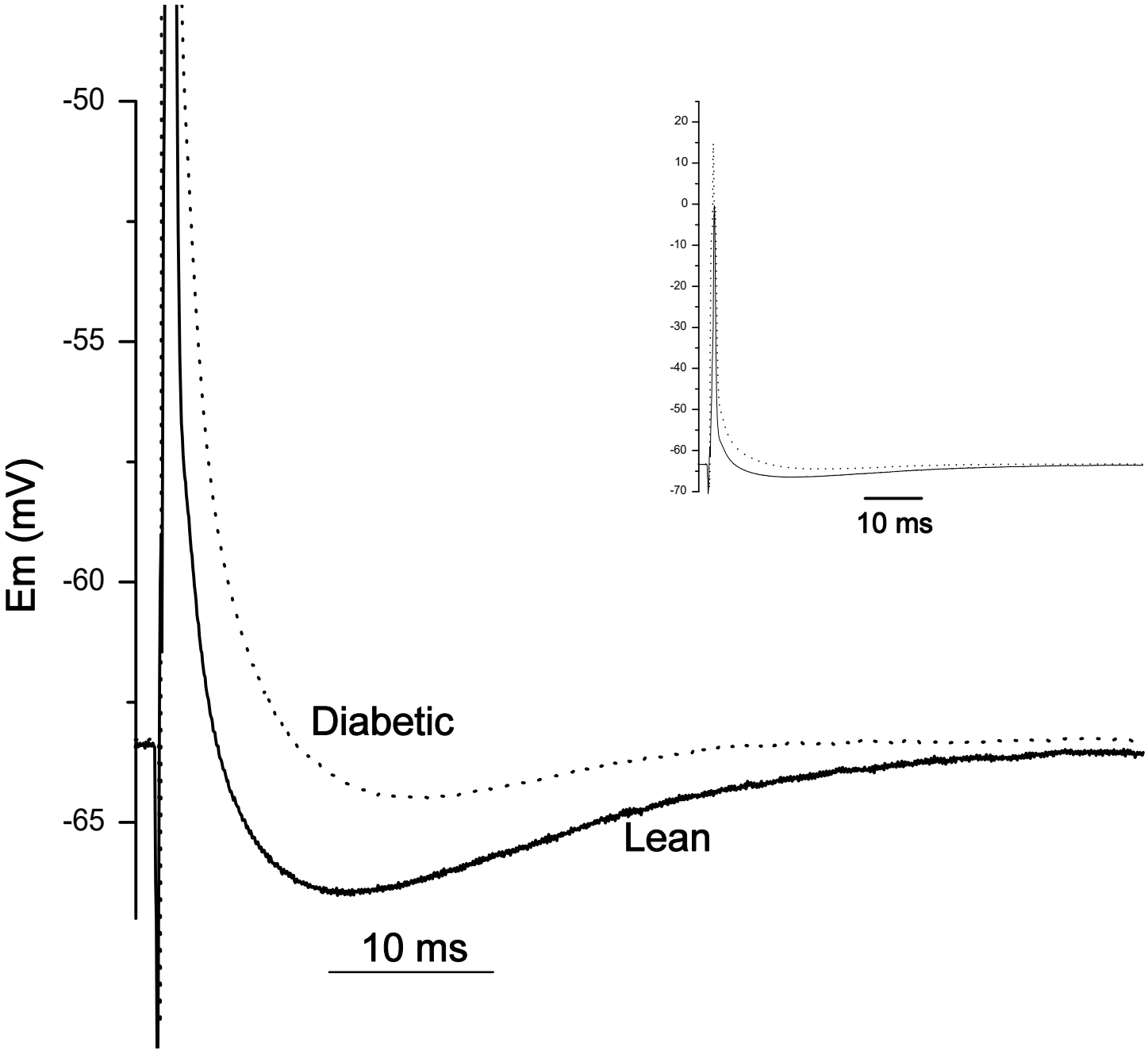
-50
-55
-60
-65
Em (mV)
Diabetic
Lean
10 ms
20
10
0
-10
-20
-30
-40
-50
-60
-70
10 ms

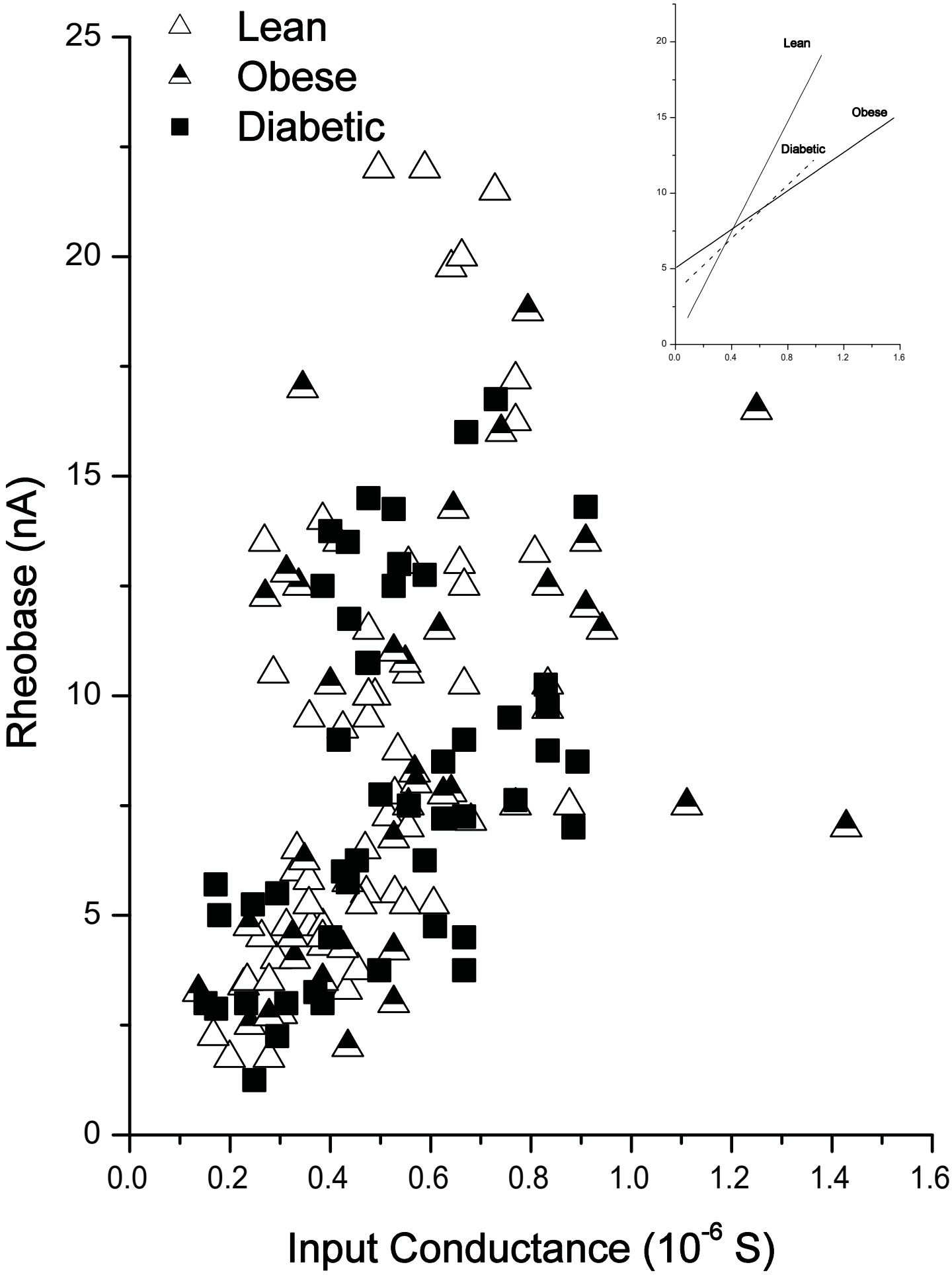
Lean
Obese
Diabetic
Rheobase (nA)
Input Conductance (10^{-6} S)
0
5
10
15
20
25
0.0
0.2
0.4
0.6
0.8
1.0
1.2
1.4
1.6
Lean
Obese
Diabetic
0
5
10
15
20
0.0
0.4
0.8
1.2
1.6

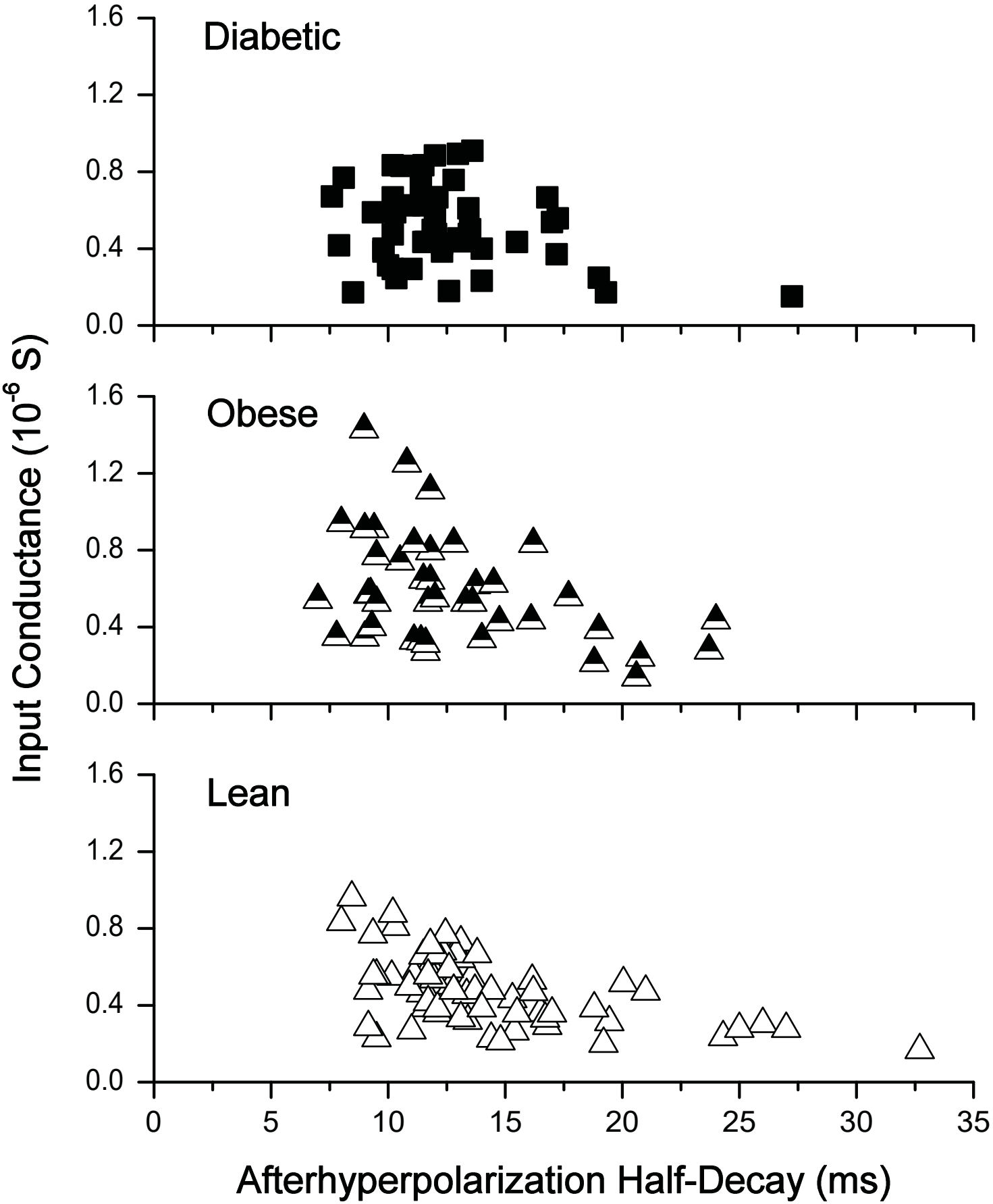
Diabetic
Obese
Lean
Input Conductance (10^{-6} S)
Afterhyperpolarization Half-Decay (ms)
0.0
0.4
0.8
1.2
1.6
0
5
10
15
20
25
30
35